Track formation in clutter using a bi-band imaging sensor

J. Dezert
ONERA, 29 Av. Division Leclerc
92320 Châtillon, France
dezert@onera.fr

T. Kirubarajan
University of Connecticut, ESE Dept.
Box U-157, Storrs, CT 06269-2157, USA
kiruba@engr.uconn.edu

Abstract - ***In this paper we present an extension of the Markov-chain-based performance evaluation technique for a bi-band two-stage sliding window cascaded logic*** $(2/2 \times m/n)$ ***for track formation in clutter. This work has been motivated by a ballistic target surveillance problem based on a bi-spectral satellite observation system. We show how to combine an AND and OR fusion decision logic within the classical performance evaluation approach and how this can result in better performance and serve as a useful tool in satellite tracking system design.***

Keywords: Track formation, performance evaluation, image fusion, cascaded logic.

1 Introduction

Surveillance of targets from infrared (IR) satellite observations is a major concern for modern defense systems, especially for the detection and tracking of dim ballistic missiles. In such systems, track formation (or track initialization) is a crucial phase. The evaluation of the reliability of the track formation process (TFP) is important because of the disastrous effects the threat can have if it is not detected and a corresponding track not initiated (miss detection of a true target). Similarly, formation of false tracks when there is no target is also undesirable (false track initiation in the absence of a target). Thus, a tool for evaluating the true track detection and false track initiation characteristics of track initiation techniques is needed. The difficulty in developing such a tool comes from the limited resolution of the IR imaging sensor, possibility of miss detection of target-originated measurements, presence of false alarms due to environmental conditions (mainly due to cloud borders) and the uncertainty about target characteristics (number of targets, their dynamics, target types, etc.). Several approaches to developing such an analysis tool have been proposed in the literature [1][3] for single-imaging (i.e., mono-band) sensors. Recent technological advances allow us to have several IR imaging sensors on the same satellite with different spectral bands in order to obtain better target detection. For such multi-band sensors no tools to evaluate the TFP exist. In this paper we develop a procedure for the evaluation of the performance of a track formation logic for bi-band sensors.

The next section briefly describes the basics of the classic performance evaluation tool developed in [3]. Extension of this method to bi-band imaging sensors is then presented in the Section 3. Comparison of track initiation performances for mono-band and bi-band systems is also presented.

2 The mono-band case

Here, we summarize the basics of the performance evaluation using the classic cascaded logic track initiation presented in [3] for mono-band sensors. This TFP is based on the following two-stage cascaded logic $(2/2 \times m/n)$ consisting of the following stages :

1. Stage 1 : After the first detection at a sampling time (or in a frame), a validation gate [2] is set up for the next sampling time (or frame of data) and a detection has to be made within this validation gate. This is the $2/2$ requirement.
2. Stage 2 : If the requirements for Stage 1 are satisfied, then gates are set up for the subsequent sampling times based on the assumed dynamic model. Detections have to be made in m out of the next n sampling times in the corresponding gates in order to initiate a new track. This is the m/n requirement.

The basic idea for the analysis of this TFP is to take into account both the probability of detection, P_d, of target-originated measurements, the false alarm probability, P_{fa}, (defined per resolution cell) as well validation gate sizes (or equivalently, the gating probability P_g). For tracking a dim ballistic target in focal plane (image plane), we assume that the target is moving in a two dimensional space with a nearly constant acceleration motion [4] when at least 3 detections are available in the detection sequence. The target state consists of position, velocity and acceleration and the (third order) state equation for sampling period T is (in each coordinate)

$$\mathbf{x}(k+1) = \mathbf{F}\mathbf{x}(k) + \Gamma v(k) \tag{1}$$

with

$$\mathbf{F} = \begin{bmatrix} 1 & T & \frac{1}{2}T^2 \\ 0 & 1 & T \\ 0 & 0 & 1 \end{bmatrix} \quad \text{and} \quad \Gamma = \begin{bmatrix} \frac{1}{2}T^2 \\ T \\ 1 \end{bmatrix} \tag{2}$$

The white process noise (assumed to be Gaussian and zero-mean) is the acceleration increment during the k-th sampling period. The covariance of the process noise multiplied by the gain Γ is $\mathbf{Q} = \Gamma\sigma_v^2\Gamma'$. The measurements are position only, with additive white noise with variance r. If only 2 detections are available, the classical nearly constant velocity model is used instead with following matrices

$$\mathbf{F} = \begin{bmatrix} 1 & T \\ 0 & 1 \end{bmatrix} \quad \text{and} \quad \Gamma = \begin{bmatrix} \frac{1}{2}T^2 \\ T \end{bmatrix} \tag{3}$$

The state covariance for each coordinate evolves according to the usual Riccati equation modified with a detection indicator $\delta(k)$ defined by

$$\delta(k) = \begin{cases} 1, & \text{if there is a detection in the gate at } k \\ 0, & \text{otherwise} \end{cases} \tag{4}$$

That is,

$$\begin{aligned} \mathbf{P}(k|k-1) &= \mathbf{F}\mathbf{P}(k-1|k-1)\mathbf{F}' + \mathbf{Q} \\ \mathbf{P}(k|k) &= (\mathbf{I} - \delta(k)\mathbf{K}(k)\mathbf{H})\mathbf{P}(k|k-1) \end{aligned}$$

where $\mathbf{I}$ is the identity matrix with appropriate dimension, $\mathbf{H}$ is the observation matrix and $\mathbf{K}(k)$ is the classical Kalman gain matrix given by

$$\mathbf{K}(k) = \mathbf{P}(k|k-1)\mathbf{H}'\mathbf{S}^{-1}(k) \tag{5}$$

with

$$\mathbf{S}(k) = \mathbf{H}\mathbf{P}(k|k-1)\mathbf{H}' + \mathbf{R} \tag{6}$$

The TFP based on a $2/2 \times m/n$ cascaded logic can be modeled by a Markov chain. At a given time k, a state $\delta_i(k)$ of the chain consists of the detection sequence indicator vector (see next section). The transition probability π_{ij} between a current state $\delta_i(k)$ of the chain and another state $\delta_j(k+1)$ depends on the detection $D(k)$ (or no detection $\bar{D}(k)$) done in the gate at time k and the detection $D(k+1)$ (or no detection $\bar{D}(k+1)$) done at time $k+1$. The number N of states of the Markov chain depends on the choice of the m/n logic.

If the origin of the detection at time $k+1$ is the true target, the probability for transitions $D(k) \to D(k+1)$ and $\bar{D}(k) \to D(k+1)$ are equal to $P_d P_g$ where P_g is a given gating probability which defines the gating size [2]. Obviously the probability for transitions $D(k) \to \bar{D}(k+1)$ and $\bar{D}(k) \to \bar{D}(k+1)$ are equal to $1 - P_d P_g$.

If the origin of the detection at time $k+1$ is a false alarm coming from a Poisson clutter with pmf

$$\mu_F(m_F) = \frac{(P_{fa}V)^{m_F}}{m_F!} e^{-P_{fa}V}$$

where P_{fa} is the false alarm probability per cell per scan (assumed to be constant) and V is the volume of the validation gate (in resolution cell units), then one has

$$P\{m_F \geq 1\} = \sum_{m_F=1}^{\infty} \mu_F(m_F) = 1 - e^{-P_{fa}V} \tag{7}$$

If we assume the probability of having more than one false alarm per gate is negligible, then one gets

$$P\{m_F \geq 1\} = 1 - e^{-P_{fa}V} \approx P_{fa}V \tag{8}$$

Hence the probability for transitions $D(k) \to D(k+1)$ and $\bar{D}(k) \to D(k+1)$ when detection is false alarm originated become now equal to $P_{fa}V(k+1)$. The probability for transitions $D(k) \to \bar{D}(k+1)$ and $\bar{D}(k) \to \bar{D}(k+1)$ become then $1 - P_{fa}V(k+1)$.

The probability of confirmation of a **target-originated sequence** (pure true track formation) is obtained by propagation of the state probability vector μ according to [3, 5]

$$\boldsymbol{\mu}(k+1) = \boldsymbol{\Pi}'\boldsymbol{\mu}(k) \tag{9}$$

where $\boldsymbol{\Pi} = [\pi_{ij}]$ is the known transition matrix of the Markov chain of the chosen cascaded-logic $2/2 \times m/n$ and $\boldsymbol{\mu}(k)$ is a N-dimensional vector for which each component $\mu_i(k)$ $(i = 1, \ldots, N)$ represents the probability that the logic is in state i at time k. N is the index of the step for which the cascaded track formation logic is valid. This step is called **acceptance step** or **confirmed status**. At the initial time $k = 0$, we have to set $\mu_i(k) = 1$. The component $\mu_N(k)$ of $\boldsymbol{\mu}(k)$ represents the cumulative probability mass function of the true track confirmation at time k and the **expected true track confirmation time** $\bar{t}_c$ is then given by

$$\bar{t}_c = E[t_c] = \sum_{k=1}^{\infty} k(\mu_N(k) - \mu_N(k-1)) \tag{10}$$

The evaluation of the false track acceptance probability of a **false-alarm-originated sequence** (pure false track formation) is a little bit more complex because it requires the computation of the volume of the gate for each time k of the TFP. Any volume $V_i(k)$ (expressed in number of resolution cells) highly depends on its detection indicator vector $\boldsymbol{\delta}_i(k)$ (and therefore on subsequent states of the chain having given rise to $\boldsymbol{\delta}_i(k)$). Mathematically, $V_i(k)$ can be computed for the two-dimensional measurement case by

$$V_i(k) = \gamma\pi\sqrt{|\mathbf{S}(\boldsymbol{\delta}_i(k))|} \tag{11}$$

where γ is the validation threshold [2] associated to the gating probability P_g and $\mathbf{S}(\boldsymbol{\delta}_i(k))$ is the innovation covariance given in (6) and corresponding to the detection sequence $\boldsymbol{\delta}_i(k)$. In such case, the propagation of the state probability vector μ is given by

$$\boldsymbol{\mu}(k+1) = \boldsymbol{\Pi}'_F\boldsymbol{\mu}(k) \tag{12}$$

where $\boldsymbol{\Pi}_F$ is the Markov transition matrix taking into account detection indicators $\boldsymbol{\delta}_i(k)$. For each time k the full transition matrix of the Markov chain must

be reevaluated because of the varying of gate volumes. The transition probability from state $\boldsymbol{\delta}_i(k)$ towards next state will then become $P_{fa}V_i(k)$ if there is a (false) detection in the validation gate at time k or $1 - P_{fa}V_i(k)$ otherwise. For a given logic which generates N steps, the initial state probability vector $\mu(0) = [\mu_1(0) \dots \mu_N(0)]'$ must be set to $\mu(0) = [1 - P_{fa}\, P_{fa}\, 0 \dots 0]'$. If the last state of the chain is obtained in p steps, the false track probability P_{FT} (the probability that a resolution cell yields an accepted false track per scan) is then given by

$$P_{FT} = P\{t_F \geq p\} = \mu_N(p) \tag{13}$$

where t_F is the time for which the acceptance state N is reached.

The average number of accepted (pure) false tracks per scan for an imaging system having N_c resolution cells is $N_c P_{FT}$ and the average false track length in sampling periods is

$$\bar{t}_F = E[t_f] = \frac{\sum_{i=2}^{N} \sum_{k=1}^{p} k\mu_i(k)}{\sum_{i=2}^{N} \sum_{k=1}^{p} \mu_i(k)} \tag{14}$$

Therefore, the expected number of false tracks at a given time which defines the processor sizing for the system design is

$$E[N_F] = N_c P_{FT} \bar{t}_F \tag{15}$$

2.1 Example

As in [3], we consider here the $2/2 \times 2/3$ cascaded logic with known parameters P_d, P_g and P_{fa}. With such track formation logic, only 8 states are required for the Markov chain description. This is summarized in the table 1. The first column of the table indicates the possible states of the Markov chain for the $2/2 \times 2/3$ logic. The second column indicates the detection indicator vector (sequence of validated measurement in the gates). The third column indicates the transition destinations following a non detection or a detection in the gate.

State	Detections	Transitions
s_1	$\boldsymbol{\delta}_1 = \emptyset$	$\bar{D} \rightarrow s_1$ or $D \rightarrow s_2$
s_2	$\boldsymbol{\delta}_2 = [1]$	$\bar{D} \rightarrow s_1$ or $D \rightarrow s_3$
s_3	$\boldsymbol{\delta}_3 = [11]$	$\bar{D} \rightarrow s_4$ or $D \rightarrow s_5$
s_4	$\boldsymbol{\delta}_4 = [110]$	$\bar{D} \rightarrow s_1$ or $D \rightarrow s_6$
s_5	$\boldsymbol{\delta}_5 = [111]$	$\bar{D} \rightarrow s_7$ or $D \rightarrow s_8$
s_6	$\boldsymbol{\delta}_6 = [1101]$	$\bar{D} \rightarrow s_1$ or $D \rightarrow s_8$
s_7	$\boldsymbol{\delta}_7 = [1110]$	$\bar{D} \rightarrow s_1$ or $D \rightarrow s_8$
s_8	$\boldsymbol{\delta}_{8a} = [11011]$	$\bar{D} \rightarrow s_8$ or $D \rightarrow s_8$
	$\boldsymbol{\delta}_{8b} = [11111]$	$\bar{D} \rightarrow s_8$ or $D \rightarrow s_8$
	$\boldsymbol{\delta}_{8c} = [11101]$	$\bar{D} \rightarrow s_8$ or $D \rightarrow s_8$

Table 1: The Markov chain for the $2/2 \times 2/3$ logic

Once this Markov chain has been generated following the scheme on figure 1, we can easily set the values π_{ij} corresponding to the possible transitions of the TFP. If we are concerned by a true target originated track, we will set

$$\pi_{11} = \pi_{21} = \pi_{36} = \pi_{45} = \pi_{51} = \pi_{61} = \pi_{71} = 1 - P_d P_g$$
$$\pi_{12} = \pi_{23} = \pi_{34} = \pi_{48} = \pi_{58} = \pi_{67} = \pi_{78} = P_d P_g$$
$$\pi_{88} = 1$$

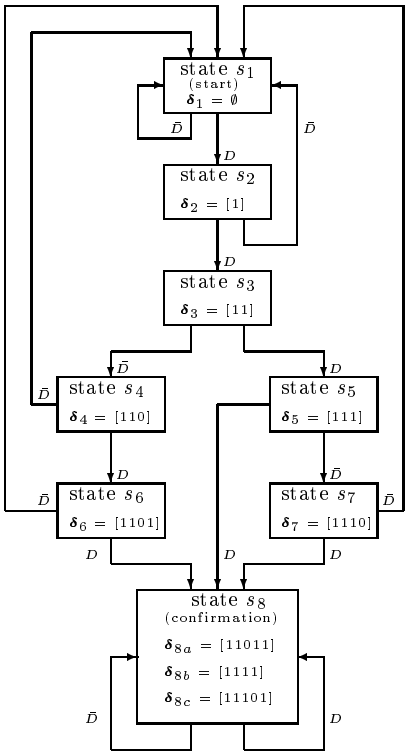

Figure 1: Markov chain for $2/2 \times 2/3$ cascaded logic

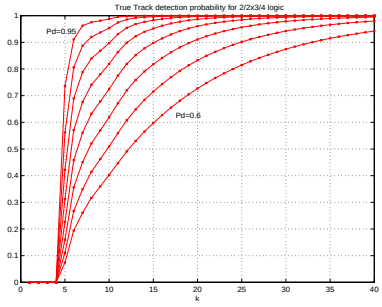

Figure 2: True Track proba P_{DT} for logic 3/4

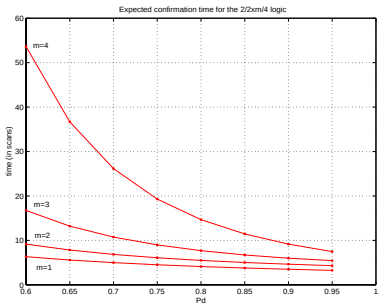

Figure 3: Average True Track Confirmation Time $\bar{t}_c$

The probabilities of detection of the true track $P_{DT} = \mu_N(k)$ for $P_d = 0.95$ to 0.6 by decreasing step of 0.05 and for the logic $2/2 \times 3/4$ are plotted on figure 2. The expected true track confirmation times $\bar{t}_c$ given by (10) for logics $2/2 \times m/4$ are plotted on figure 3.

The table 2 shows the number of states involved in the generation of the Markov chain for different couples of (m, n) for a $2/2 \times m/n$ logic for the mono-band case.

	n=3	n=4	n=5	n=6	n=7	n=8	n=9	n=10
m=2	8	12	17	23	30	38	47	57
m=3	6	12	22	37	58	86	122	167
m=4		7	17	37	72	128	212	332
m=5			8	23	58	128	254	464
m=6				9	30	86	212	464
m=7					10	38	122	332
m=8						11	47	167
m=9							12	57
m=10								13

Table 2: Number of states for logic $2/2 \times m/n$

For evaluation of the false-alarm-originated track probability $P_{FT}(k) = \mu_N(p)$, the major difficulty is to evaluate the varying gate volumes depending of the detection indicator vector associated to every possible state of the Markov chain. In this work, because we were concerned by ballistic missile track formation in 2D focal plane of imaging sensor, we have used the constant velocity model (CV) whenever the number of detections present in the detection indicator vector was less than 3; otherwise the nearly constant acceleration model (CA) has been used for evaluation of gate volumes. When the CA model can be used, the initial covariance matrix $\mathbf{P}(0|0)$ has been estimated by the classical polynomial fitting technique [4] to get a better precision; The following parameters were used :

1. The measurement precision in x and y expressed in resolution cell units has been taken to $r_x = r_y = 1$ (i.e., 1 pixel).
2. The gating probability P_g was 0.99 (which yields to take $\gamma = 9.21$ as validation threshold for 2D measurement).
3. An assumption of a maximum velocity of 10 cells/scan in each direction is done for initial time. This leads to have $V_2 \approx 400$ pixels.

Table 3 presents the resulting false track probability, the average length (in scans) of a false track, and the expected number of false tracks at a given time for various false alarm densities and logic parameters m/n for a $N_c = 1000 \times 1000$ imaging sensor.

3 The bi-band case

In this section, we extend the analysis developed in [3] to the bi-band case and show how fusion of bi-band data can be used efficiently in the TFP. The bi-band sensor provides two images in two different spectral bands of the same observed scene with the same resolution (i.e., the same number of pixels for the same

	$P_{fa} = 10^{-5}$			$P_{fa} = 10^{-3}$		
	P_{FT}	t_f	$E[N_F]$	P_{FT}	t_f	$E[N_F]$
2/3	4.97e-12	1.51	7.55e-06	1.20e-04	2.40	289.84
3/3	6.99e-16	1.00	7.00e-10	3.75e-06	1.24	4.67
2/4	2.61e-11	2.04	5.33e-05	2.84e-04	2.87	820.05
3/4	1.18e-14	1.51	1.80e-08	2.93e-05	2.52	74.17
4/4	1.18e-18	1.00	1.18e-12	5.87e-07	1.22	0.72
2/5	2.61e-11	2.57	6.72e-05	2.84e-04	3	854.85
3/5	8.12e-14	2.04	1.65e-07	9.78e-05	3.67	359.48
4/5	2.24e-17	1.51	3.41e-11	5.61e-06	2.42	13.59
5/5	1.80e-21	1.00	1.80e-15	8.28e-08	1.22	0.10
2/6	2.61e-11	3	7.84e-05	2.84e-04	3	854.85
3/6	3.75e-13	2.57	9.65e-07	2.01e-04	4.39	887.12
4/6	1.89e-16	2.04	3.86e-10	2.46e-05	3.96	97.90
5/6	3.86e-20	1.51	5.87e-14	9.55e-07	2.31	2.21
6/6	2.63e-24	1.00	2.63e-18	1.12e-08	1.22	0.013
2/7	2.61e-11	3	7.84e-05	2.84e-04	3	854.85
3/7	1.36e-12	3.11	4.29e-06	3.04e-04	4.80	1460.85
4/7	1.08e-15	2.57	2.80e-09	6.96e-05	5.61	391.05
5/7	3.89e-19	2.04	7.94e-13	5.28e-06	3.80	20.11
6/7	6.39e-23	1.51	9.70e-17	1.54e-07	2.27	0.35
7/7	3.78e-27	1.00	3.79e-21	1.51e-09	1.22	1.84e-03

Table 3: False Track Probability and Average False Track length for logics $2/2 \times m/3$ to $2/2 \times m/7$

image). There is no alignment/registration errors between the two images. Basically the image fusion approach or local track fusion approach can both be used to solve the bi-band track formation problem.

3.1 Bi-band image fusion approach

Two techniques could be developed within this image fusion approach. The first (post-detection) technique is to merge the two primary spectral band signals into a single signal to form a new image. Then, signal thresholding techniques can be applied on this fused image for target detection. The second (pre-detection) technique consists of applying detection thresholding techniques on each spectral image and merge the thresholded images into a single image using classical AND/OR logic-based pixel fusion. Once the single fused image is available, the classical mono-band technique described in [3] can be used for TFP. With these two image fusion options, one does not have to develop a new TFP specific to bi-band data at all. That is, the bi-band problem is reduced to a mono-band one by the pixel-based fusion. The main difficulty in this approach is the development of efficient and optimal image fusion techniques.

3.2 Bi-band local track fusion approach

An alternative to the image fusion described above is local track fusion. It consists of using separately the two thresholded images to develop a new bi-band TFP based on optimal track fusion and AND/OR fusion rule for gating. There is no need to use image/pixel fusion in this approach, which greatly simplifies its implementation. In this paper we focus on local track fusion and develop a TFP specific to bi-band imaging sensors.

3.2.1 The AND fusion rule

The true TFP for the bi-band imaging sensor follows exactly the true TFP described for the mono-band case. We have to consider the same pixel, say p_{ij}, for both images for spectral bands B_1 and B_2 and we denote by D_1 the target detection for p_{ij} in band B_1 and D_2 the target detection for p_{ij} in band B_2. In others words if the values of pixels p_{ij} in both images

is one, then we will say that there is a target detection at this pixel otherwise if one of the pixels value is zero (or both) (i.e. one has $\bar{D}_1 D_2$, $D_1 \bar{D}_2$ or $\bar{D}_1 \bar{D}_2$) we will consider that there is no bi-band target detection. This is the AND fusion rule. The bi-band target detection indicator at time k, denoted $\delta(k)$, can take the possible values depending on the target detection in bands B_1 and B_2 :

$$\begin{aligned}
\boldsymbol{\delta}(k) &= [1\ 1]' \quad \text{if} \quad D_1 D_2 \quad \text{(AND detection)} \\
\boldsymbol{\delta}(k) &= [0\ 1]' \quad \text{if} \quad \bar{D}_1 D_2 \quad \text{(no AND detection)} \\
\boldsymbol{\delta}(k) &= [1\ 0]' \quad \text{if} \quad D_1 \bar{D}_2 \quad \text{(no AND detection)} \\
\boldsymbol{\delta}(k) &= [0\ 0]' \quad \text{if} \quad \bar{D}_1 \bar{D}_2 \quad \text{(no AND detection)}
\end{aligned}$$

The transition π_{ij} between states s_i and s_j of the Markov chain of the bi-band TFP is governed by the occurrence or non-occurrence of the bi-band detection event. The state transition probability will be

$$\begin{aligned}
P_{d1} P_{g1} P_{d2} P_{g2} \quad &\text{if} \quad D_1 D_2 \\
(1 - P_{d1} P_{g1}) P_{d2} P_{g2} \quad &\text{if} \quad \bar{D}_1 D_2 \\
P_{d1} P_{g1} (1 - P_{d2} P_{g2}) \quad &\text{if} \quad D_1 \bar{D}_2 \\
(1 - P_{d1} P_{g1)(1-} P_{d2} P_{g2}) \quad &\text{if} \quad \bar{D}_1 \bar{D}_2
\end{aligned}$$

P_{d1},P_{d2} are the target detection probabilities for spectral bands B_1 and B_2. P_{g1} and P_{g2} are the gating probabilities (usually $P_{g1} = P_{g2} \equiv P_g$).

As for the mono-band case, the probability of confirmation of a **bi-band target-originated sequence** (pure true track formation) is obtained by propagation of the state probability vector μ according to (9). The **expected true track confirmation time** $\bar{t}_c$ is also defined as previously in (10).

The evaluation of the bi-band false track acceptance probability of a **false-alarm-originated sequence** (pure false track formation) is more complex because it requires, for each time k, the computation of the volumes of the gates $V_1(k)$ and $V_2(k)$ for spectral bands B_1 and B_2 of the TFP. Every gate volume (expressed in number of resolution cells) associated to a given state highly depends on previous states of the Markov chain and the sequence of detection indicators $\boldsymbol{\delta}$. Here are the steps required for evaluation of such gate volumes :

For $t = 1$ to current time k do :

$$\begin{aligned}
\mathbf{P}^- \triangleq \mathbf{P}(t|t-1) &= \mathbf{F}' \mathbf{P}(t-1|t-1) \mathbf{F}' + \mathbf{Q} \\
\mathbf{S}_1 &= \mathbf{H}_1 \mathbf{P}^- \mathbf{H}_1' + \mathbf{R}_1 \\
\mathbf{P}_1(t|t) &= \mathbf{P}^- - \delta_1 \mathbf{P}^- \mathbf{H}_1' \mathbf{S}_1^{-1} \mathbf{H}_1 \mathbf{P}^- \\
\mathbf{S}_2 &= \mathbf{H}_2 \mathbf{P}^- \mathbf{H}_2' + \mathbf{R}_2 \\
\mathbf{P}_2(t|t) &= \mathbf{P}(t|t-1) - \delta_2 \mathbf{P}^- \mathbf{H}_2' \mathbf{S}_2^{-1}(t) \mathbf{H}_2 \mathbf{P}^- \\
\mathbf{P}(t|t) &= [\mathbf{P}_1^{-1}(t|t) + \mathbf{P}_2^{-1}(t|t) - \mathbf{P}^{-1}(t|t-1)]^{-1}
\end{aligned}$$

Derivation of gate volumes V_1 and V_2 for time k :

$$V_1 = \gamma \pi \sqrt{|\mathbf{S}_1(k)|} \quad \text{and} \quad V_2 = \gamma \pi \sqrt{|\mathbf{S}_2(k)|}$$

where indexes 1 and 2 correspond to bands B_1 and B_2 respectively and γ is the validation threshold associated to the gating probability P_g (we assume here that $P_{g1} = P_{g2} \equiv P_g$). $\delta_1(t)$ and $\delta_2(t)$ are the components of bi-band detection indicator $\boldsymbol{\delta}(t)$.

The propagation of the state probability vector μ is given by (12). At each time k the transition matrix of the Markov chain must be reevaluated because of the varying of gate volumes. According to (8), the transition probability between states entering into Π_F transition matrix are given by :

$$\begin{aligned}
P_{fa1} V_1(k) P_{fa2} V_2(k) \quad &\text{if} \quad D_1 D_2 \\
(1 - P_{fa1} V_1(k)) P_{fa2} V_2(k) \quad &\text{if} \quad \bar{D}_1 D_2 \\
P_{fa1} V_1(k) (1 - P_{fa2} V_2(k)) \quad &\text{if} \quad D_1 \bar{D}_2 \\
(1 - P_{fa1} V_1(k)) (1 - P_{fa2} V_2(k)) \quad &\text{if} \quad \bar{D}_1 \bar{D}_2
\end{aligned}$$

For a given logic which generates N steps, the initial state probability vector $\mu(0) = [\mu_1(0) \ldots \mu_N(0)]'$ must be set to $\mu(0) = [1 - P_{fa1} P_{fa2}\ P_{fa1} P_{fa2}\ 0 \ldots 0]'$. The bi-band false track probability P_{FT} and the expected number of false tracks at a given time are respectively given, as for mono-band case, by (13) and (14). The expected number of false tracks at a given time is also given by (15).

The table 4 shows the number of states involved in the generation of the Markov chain for different couples of (m, n) for a $2/2 \times m/n$ bi-band track formation cascaded logic based on AND fusion rule.

	n=3	n=4	n=5	n=6
m=2	14	50	185	671
m=3	6	24	114	519
m=4		7	37	217
m=5			8	53
m=6				9

Table 4: Number of states for bi-band logic $2/2 \times m/n$ based on AND fusion

By comparison of this table with table 2, we see that the dimension of Markov Chain for a given m/n logic (with $m < n$) logic increases significantly when using a bi-band imaging sensor.

Example

To illustrate the bi-band TFP based on AND fusion rule, we consider the very simple $2/2 \times 2/3$ cascaded logic. D_1 and D_2 denote the detection (if any) in the validation gates for spectral bands B_1 and B_2. The non detection events are respectively denoted $\bar{D}_1$ and $\bar{D}_2$. The Markov chain of this bi-band cascaded logic requires 14 states (only 8 states were necessary for the mono-band case) according to the figure 4.

Simulations results for the AND fusion rule

In our simulations, the target detection probabilities P_{d1} and P_{d2} have been assumed the same and constant

with time. The resulting probabilities of detection of the true track $P_{DT} = \mu_N(k)$ for $P_{d1} = P_{d2} = 0.95$ to 0.6 (by step 0.05) for the logic $2/2 \times 3/4$ are plotted on figure 5. The (true track) Markov chain generation has been implemented according to the scheme illustrated on figure 4.

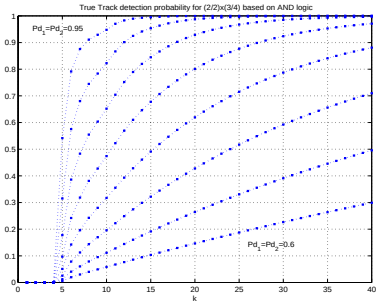

Figure 5: True Track probabilities P_{DT} for different cascaded logics based on AND fusion

Comparison of figures 5 and 2 shows that True Track probabilities obtained by bi-band TFP based on AND fusion logic are worst than those obtained by the TFP for the mono-band case. This result is only to be expected since the AND fusion logic is a very strong constraint for the cascaded logic. Table 5 presents the resulting false track probability, the average length (in scans) of a false track, and the expected number of false tracks at a given time for various false alarm densities and logic parameters m/n for a bi-band $N_c = 1000 \times 1000$ imaging sensor. We can see now by direct comparison with table 3 that performances of false track formation process are substantially far better than for the monoband case. So if the designer wants to reduce the false track acceptance probability for a given $2/2 \times m/n$ logic, he will definitely have to choose for the bi-band imaging sensor.

	$P_{fa} = 10^{-5}$			$P_{fa} = 10^{-3}$		
	P_{FT}	t_f	$E[N_F]$	P_{FT}	t_f	$E[N_F]$
2/3	3.76e-24	1.50	5.64e-18	2.66e-09	1.97	5.24e-03
3/3	2.89e-32	1.00	2.89e-26	1.12e-12	1.01	1.13e-06
2/4	6.02e-23	2.00	1.20e-16	1.84e-08	2.73	5.03e-02
3/4	6.01e-30	1.50	9.03e-24	4.28e-11	1.90	8.15e-05
4/4	3.62e-38	1.00	3.62e-32	1.26e-14	1.01	1.27e-08
2/5	5.613e-22	2.50	1.40e-15	4.1551e-08	3.32	0.137
3/5	1.32e-28	2.00	1.40e-15	4.36e-10	2.65	0.137
4/5	7.55e-36	1.50	1.13e-29	5.33e-13	1.89	1.01e-06
5/5	4.07e-44	1.00	4.07e-38	1.28e-16	1.01	1.29e-10
2/6	3.54e-21	3.00	1.06e-14	5.63e-08	3.69	0.20
3/6	1.71e-27	2.50	4.29e-21	2.10e-09	3.62	7.62e-03
4/6	2.13e-34	2.00	4.27e-28	7.26e-12	2.53	1.83e-05
5/6	8.66e-42	1.50	1.30e-35	6.04e-15	1.89	1.14e-08
6/6	4.39e-50	1.00	4.39e-44	1.25e-18	1.01	1.26e-12

Table 5: False Track Probability and Average False Track length for bi-band logics $2/2 \times m/3$ to $2/2 \times m/6$ based on AND fusion rule

3.2.2 The OR fusion rule

As previously, we consider the same pixel, say p_{ij}, for both images for spectral bands B_1 and B_2 and we denote by D_1 the target detection for p_{ij} in band B_1 and D_2 the target detection for p_{ij} in band B_2. Since we use now the OR fusion rule, the bi-band target detection occurs if *at least* one detection occurs (i.e., one of the pixels p_{ij} has taken the value 1) in a spectral band. The bi-band target detection indicator $\delta(k)$ corresponding to the OR fusion rule can take the following values depending on the target detection in bands B_1 and B_2 :

$$\begin{aligned}
\delta(k) = 1 \boldsymbol{\delta}(k) = [1\ 1]' \quad &\text{if} \quad D_1 D_2 \quad \text{(OR detection)} \\
\boldsymbol{\delta}(k) = [0\ 1]' \quad &\text{if} \quad \bar{D}_1 D_2 \quad \text{(OR detection)} \\
\boldsymbol{\delta}(k) = [1\ 0]' \quad &\text{if} \quad D_1 \bar{D}_2 \quad \text{(OR detection)} \\
\boldsymbol{\delta}(k) = [0\ 0]' \quad &\text{if} \quad \bar{D}_1 \bar{D}_2 \quad \text{(no OR detection)}
\end{aligned}$$

The transition π_{ij} between states s_i and s_j of the Markov chain of the bi-band TFP is governed by the occurrence or non-occurrence of the bi-band detection event and will be given by

$$\begin{aligned}
P_{d1} P_{g1} P_{d2} P_{g2} \quad &\text{if} \quad D_1 D_2 \\
(1 - P_{d1} P_{g1}) P_{d2} P_{g2} \quad &\text{if} \quad \bar{D}_1 D_2 \\
P_{d1} P_{g1} (1 - P_{d2} P_{g2}) \quad &\text{if} \quad D_1 \bar{D}_2 \\
(1 - P_{d1} P_{g1)(1-} P_{d2} P_{g2}) \quad &\text{if} \quad \bar{D}_1 \bar{D}_2
\end{aligned}$$

The probability of confirmation of a **bi-band target-originated sequence** (pure true track formation) is still obtained by propagation of the state probability vector μ according to (9) and the **expected true track confirmation time** $\bar{t}_c$ is given by (10). The evaluation of the bi-band false track acceptance probability of a **false-alarm-originated sequence** (pure false track formation) is done as described previously for the AND fusion rule. The bi-band false track probability P_{FT}, the expected number of false tracks at a given time and the expected number of false tracks are respectively given, as for mono-band case, by (13), (14) and (15). The table 6 shows the number of states involved in the generation of the Markov chain for different couples of (m, n) for a bi-band $2/2 \times m/n$ TFP based on OR fusion rule. For $m \geq 4$ and $n \geq 5$, our personal computer was however unable to compute the huge number of states involved in Markov chain of the TFP due to memory limitations. Such cases are denoted by OM (Out of memory) in the table. For practical applications, we point out that the OR fusion rule for the bi-band TFP is very memory greedy and time consuming with respect to AND fusion rule.

	n=3	n=4	n=5
m=2	104	194	311
m=3	122	428	1004
m=4		365	OM
m=5			OM

Table 6: Number of states for bi-band logic $2/2 \times m/n$ based on OR fusion rule

We conclude that the dimension of Markov Chain of the TFP based on OR fusion rule for a given m/n logic increases drastically with respect to bi-band TFP based on AND fusion rule and mono-band case. This greedy memory constraint can be a severe limitation of

application of this logic to practical implementation. However, results show that a big improvement of the true track probability acceptance is obtained by this approach over the mono-band and bi-band AND logic.

Example

We consider again the very simple $2/2 \times 2/3$ cascaded logic. The Markov chain of this bi-band cascaded logic using OR fusion rule requires 104 states (only 8 states were necessary for the mono-band case and 14 states for bi-band TFP based on AND fusion rule). The TFP is summarized by the figure 6.

Simulations results for the OR fusion rule

The probabilities of detection of the true track $P_{DT} = \mu_N(k)$ for $P_{d1} = P_{d2} = 0.95$ to 0.6 and for the logic $2/2 \times 3/4$ are plotted on figure 7. The generation of the Markov chain has been implemented according to the scheme illustrated on figure 6.

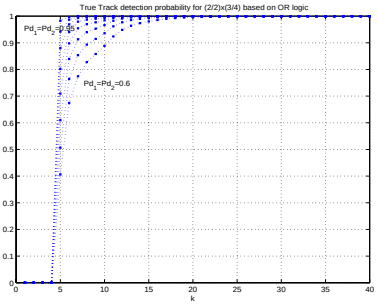

Figure 7: True Track proba P_{DT} for logic $2/2 \times 3/4$ based on OR fusion

Comparison of figures 7 and 2 show that probabilities of true track acceptance obtained by bi-band TFP based on OR fusion logic are really far better than those obtained by the TFP for the mono-band case and the bi-band TFP using AND fusion rule. Conversely, the performance of false track acceptance are now worst than for the mono-band or bi-band TFP using AND fusion rule as one can check on following table

	$P_{fa} = 10^{-5}$			$P_{fa} = 10^{-3}$		
	P_{FT}	t_f	$E[N_F]$	P_{FT}	t_f	$E[N_F]$
2/3	7.80e-11	1.55	1.21e-04	6.13e-04	6.93	4252.44
3/3	2.21e-14	1.00	2.22e-08	5.63e-05	13.00	732.87 =
2/4	4.03e-10	2.13	8.6074e-04	1.14e-03	7.82	8927.30
3/4	3.72e-13	1.53	5.72e-07	2.66e-04	22.70	6059.80
4/4	7.53e-17	1.00	7.55e-11	1.57e-05	32.89	516.99
2/5	1.38e-09	2.75	38.09e-04	12.75e-04	7.99	10198.20

Table 7: False Track proba and Average False Track length for bi-band logics based on OR fusion rule

4 Conclusions

In this paper, an extension of cascaded logic track formation for bi-band imaging sensors was presented. The proposed performance evaluation technique avoids the need for extensive simulations and is applicable to both AND/OR fusion rules on the two images. This new technique can be used to select logic parameters based on the desired true track detection and false track acceptance probabilities. It was shown that for a given bi-band $2/2 \times m/n$ cascaded logic, the probability of true track acceptance can be improved by choosing the OR fusion rule whereas the probability of false track acceptance can be reduced by choosing the AND fusion rule. It is not possible to increase the true track probability and decrease the false track probability simultaneously by using the same fusion rule.

References

[1] Barniv Y., "Dynamic Programming Algorithm for Detecting Dim Moving Targets", *in Multitarget-Multisensor Tracking: Advanced Applications*, Artech House (Y. Bar-Shalom Ed.,pp. 85-154, (1990).

[2] Bar-Shalom Y., Fortmann T.E., "Tracking and Data Association", *Academic Press*, (1988).

[3] Bar-Shalom Y., Chang K.C., Shertukde H.M. "Performance Evaluation of a Cascaded Logic for Track Formation in Clutter", *IEEE Trans. AES*, vol. 25, no 6, pp. 873-878, (1986).

[4] Bar-Shalom Y., Li X.R., "Estimation and Tracking: Principles,Techniques, and Software", *Artech House*, (1993).

[5] Bar-Shalom Y., Li X.R., "Multitarget-Multisensor Tracking: Principles and Techniques", *YBS Publishing*, (1995).

[6] Castella F.R., "Sliding Window Detection Probabilities", *IEEE Trans. AES*, vol. 12, pp. 815-819, (1976).

[7] Chong C.Y., "Hierarchical Estimation", *Proceedings of MIT/ONR C3 Workshop*, Monterey, CA,1979

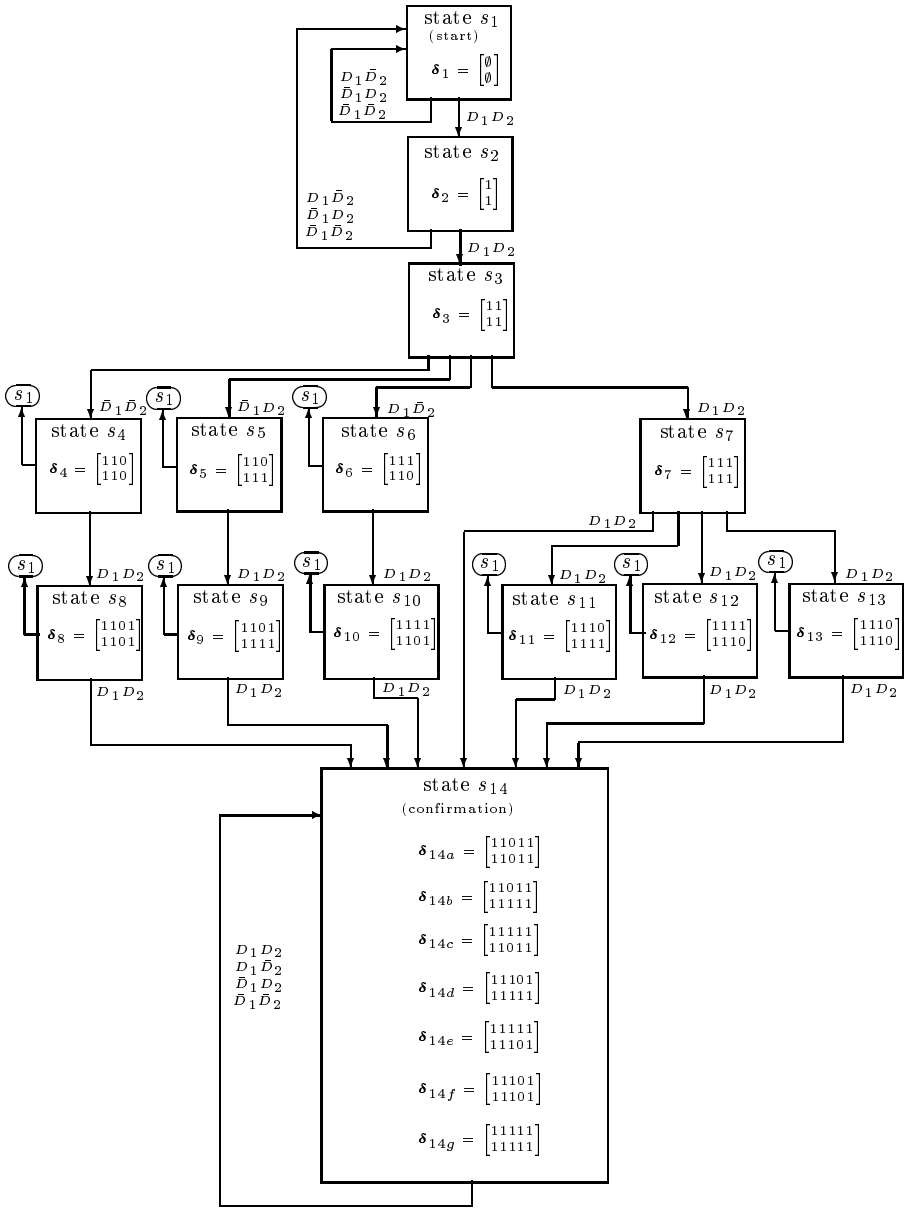

Figure 4: Bi-band Markov chain for $2/2 \times 2/3$ cascaded AND logic

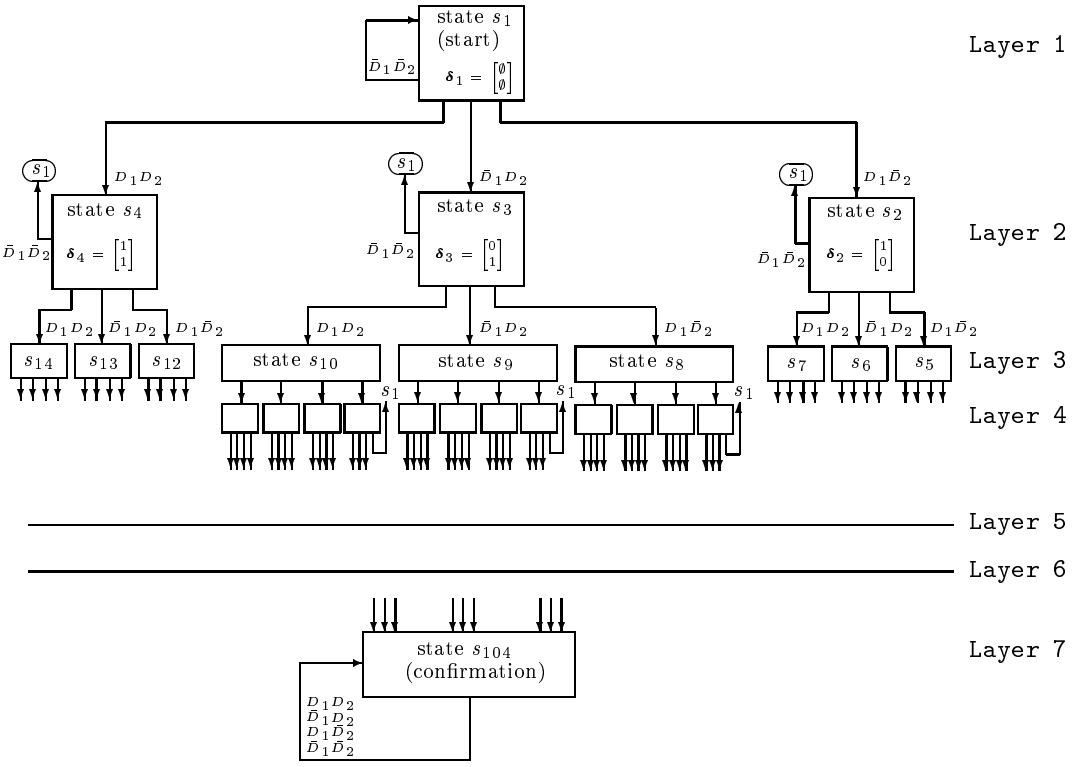

Figure 6: Bi-band Markov chain for $2/2 \times 2/3$ cascaded OR logic